Journal of Southeast University (English Edition) Vol. 32, No. 1, pp. 51 - 57 Mar. 2016 ISSN 1003—7985

Stability analysis of ellipse-like suspen-dome structures with low rise-span ratio

Ding Mingmin Luo Bin Chen Xiangnan Guo Zhengxing Guan Dongzhi

(Key Laboratory of Concrete and Pre-stressed Concrete Structures of Ministry of Education, Southeast University, Nanjing 210096, China)
(National Pre-Stressed Engineering Center of China, Southeast University, Nanjing 210096, China)

Abstract: To investigate the effects of initial geometric imperfection and material nonlinearity on the stability analysis of the suspen-dome, the steel roof of Jiangsu Culture Sports Center Gymnasium was utilized as a numerical model, and modal analyses were performed. Then, linear buckling analysis, geometric nonlinear stability analysis, geometric nonlinear stability analysis with initial imperfection, and double nonlinear analysis considering material nonlinearity and geometric nonlinearity were discussed in detail to compare the stability performance of the ellipse-like suspen-dome and the single-layer reticulated shell. The results show that the cable-strut system increases the integrity of the suspen-dome, and moderates the sensibility of the single-layer reticulated shell to initial geometric imperfection. However, it has little influence on integral rigidity, fundamental vibration frequencies, linear ultimate live loads, and geometric nonlinear ultimate live loads without initial imperfection. When considering the material nonlinearity and initial imperfection, a significant reduction occurs in the ultimate stability capacities of these two structures. In this case, the suspen-dome with a low rise-span ratio is sensitive to the initial imperfection and material nonlinearity. In addition, the distribution pattern of live loads significantly influences the instability modes of the structure, and the uniform live load with full span is not always the most dangerous case.

Key words: suspen-dome; single-layer reticulated shell; ellipse-like; stability analysis; initial geometric imperfection; geometric nonlinearity; material nonlinearity

DOI: 10.3969/j.issn.1003 - 7985.2016.01.010

The suspen-dome is a new-type hybrid system of space grid structures, which was put forward based on the concept of combining tensegrity systems with the reticulated shell[1-2]. The suspen-dome is characterized by simple configuration, high rigidity and large spanning ability, which has been successfully applied to nearly 20 projects all over the world[3]. Most projects are circular or ellipse suspen-domes, for example, Hikarigaoka Dome and Fureai Dome in Japan[2,4], Jinan Olympic Sports Center[5], Chiping Gymnasium[6] and Wuhan Sports Center Gymnasium[7]. More recently, in order to meet the requirements of architectural function, ellipse-like suspen-domes have been widely used in civil engineering projects, such as Dalian Sports Center Gymnasium[8] and Jiangsu Culture Sports Center Gymnasium.

A typical suspen-dome structure consists of a single-layer reticulated shell and a lower cable-strut system. Due to the instability of the upper reticulated shell, the structural bearing capacity sharply decreases, resulting in the destruction of the entire structure. Thus, it is necessary to investigate the stability performance of suspen-domes. In recent years, many researchers have conducted intensive research in this area. Kang et al.[9] addressed the numerical analysis and design issues of suspen-dome structural systems. Zhou et al.[10] assumed the initial curvature of members as half-wave sinusoids, and derived a stiffness equation of imperfect beam elements to investigate the effects of member geometric imperfection on nonlinear buckling analysis. Liu et al.[11] developed an improved method, based on B-R criterion, to evaluate the dynamic stability of suspen-domes, and pointed out that the rise-span ratio has different effects on dynamic stability. However, the existing research mainly focuses on geometric nonlinearity and initial geometric imperfection[12], with few concerns on material nonlinearity. Relevant provisions in Technical Specification for Space Frame Structures[13] indicate that large or complex reticulated structures should consider elastic-plastic material properties during stability analysis.

The objective of this paper is to analyze the stability performance of ellipse-like suspen-dome structures, taking Jiangsu Culture Sports Center Gymnasium as a numerical example. In this paper, the effects of initial geometric imperfection and material nonlinearity on the stability analysis are studied, and a comparison of the suspen-dome and the single-layer reticulated shell is performed to verify the function of the bottom cable-strut system.

Received 2015-07-23.

Biographies: Ding Mingmin (1989—), male, graduate; Luo Bin (corresponding author), male, doctor, professor, seurobin@seu.edu.cn.

Foundation items: The National Key Technology R&D Program of China (No. 2012BAJ03B06), the National Natural Science Foundation of China (No. 51308105), the Priority Academic Program Development of Jiangsu Higher Education Institutions (PAPD), the Fundamental Research Funds for the Southeast University (No. KYLX_0152, SJLX_0084, KYLX_0149).

Citation: Ding Mingmin, Luo Bin, Chen Xiangnan, et al. Stability analysis of ellipse-like suspen-dome structures with low rise-span ratio [J]. Journal of Southeast University (English Edition), 2016, 32(1): 51 - 57. DOI: 10.3969/j.issn.1003 - 7985.2016.01.010.

1 Engineering Background

An ellipse-like suspen-dome is used as the roof of Jiangsu Culture Sports Center Gymnasium. The length of the longitudinal span is 103.5 m, the length of the lateral span is 76.5 m, the vector height is 11.4 m, the longitudinal rise-span ratio is 1/9.1, the lateral rise-span ratio is 1/6.7, and the projection area is 3.65×10^4 m^2. The roof system is shown in Fig. 1.

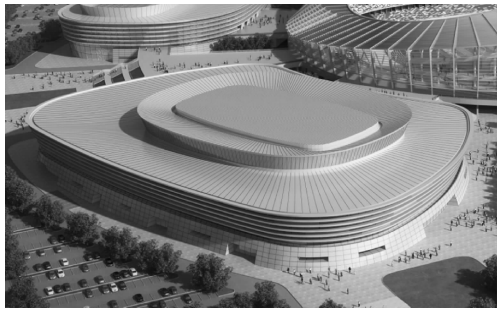

Fig. 1 Three-dimensional map of Jiangsu Culture Sports Center Gymnasium

Fig. 2 displays the plane view of a single-layer lattice shell. In Fig. 2, the upper Kiewitt reticulated shell (K8) consists of six ring components in both radial and ring directions. The shape of the single-layer lattice shell is similar to ellipse with arcs of two different radii, and the whole structure is fixed on rigid concrete columns by 30 hinged supports. The single-layer lattice shell consists of radial components and ring components. The radial components are set to be rectangular tubes with the specification of 400 mm × 400 mm × 14 mm, and the detailed component specifications of the ring components are listed in Tab. 1.

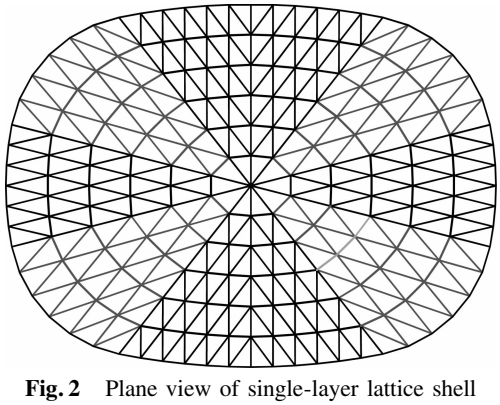

Fig. 2 Plane view of single-layer lattice shell

Tab. 1 Component specification of ring components

Ring No.	1 to 3	4 to 5	6
Ring component	Φ299 mm × 16 mm	Φ351 mm × 16 mm	Φ800 mm × 20 mm

The bottom cable-strut system consists of three ring oblique rods, two cable hoops, and several struts. Steel tubes are used as the struts and they are hinged at both ends. Oblique cables are divided into five patterns with the sectional dimensions of Φ130 mm, Φ100 mm, Φ70 mm, Φ50 mm and Φ30 mm, respectively. Cable hoops are divided into two patterns with the sectional dimensions of Φ170 mm and Φ85 mm, respectively.

2 Establishment of Finite Element Model

We use ANSYS to build the finite element model of the structure. Beam188 is selected to simulate reticulated shell components, and Link8 is chosen to simulate struts and cables. Mass21 is utilized to simulate the concentrated load on the roof.

In order to improve the accuracy of simulations, stress stiffening, geometric nonlinearity and material nonlinearity are taken into account in the calculation. In addition, we choose the Newton-Raphson method as the iteration method in this numerical analysis. The elastic modulus of cables is 160 GPa, and the one of the other components is 206 GPa.

Vertical load consists of three parts, uniform dead load, uniform live load on the roof and concentrated live load on joints. As for the uniform dead load, the weight of structure components is equivalent to 0.51 kN/m^2, and the uniform load on the roof is equivalent to 0.47 kN/m^2. The uniform live load on the roof is equivalent to 0.50 kN/m^2. Moreover, the concentrated live load at the cross joints of ring components from the first inner ring to the third inner ring is equivalent to 4.5, 3.0, and 1.5 kN, respectively.

We use the method of "adding live load by steps" to find the ultimate load of the whole structure. During the analysis, three live load combinations are taken into account: full-span arrangement, longitudinal half-span arrangement and lateral half-span arrangement. They are illustrated in Fig. 3.

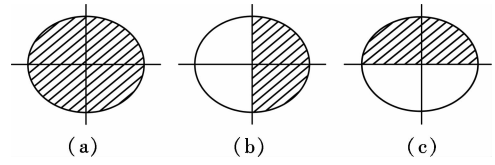

Fig. 3 Live load arrangements. (a) Full-span; (b) Longitudinal half-span; (c) Lateral half-span

3 Modal Analysis

Before modal analysis, we have finished the geometric nonlinear static analysis under the equilibrium state (the weight of the structure, dead load on the roof and initial pretension). During the vibration analysis, we use the LANB method to calculate the generalized eigenvalues of vibration modals.

Tab. 2, Fig. 4 and Fig. 5 display the frequencies of the first twelve orders, the vibration modes and the vibration mode-frequency curves of the ellipse-like suspen-dome and single-layer reticulated shell, respectively. The re-

sults are shown as follows.

1) The frequencies of the ellipse-like suspen-dome and single-layer reticulated shell are high and almost equivalent. The varying patterns of their mode-frequency curves are basically equivalent as well. This indicates that the bottom cable-strut system has little effect on the modal analysis.

2) The fundamental vibration frequencies of the suspen-dome and single-layer reticulated shell are 1.75 and 1.77 Hz, respectively, and the fundamental periods are 0.57 and 0.56 s, respectively. The results show that the fundamental vibration frequencies are relatively large, which means that the ellipse-like suspen-dome and single-layer reticulated shell have relatively large integral rigidity.

3) The basic vibration modes of the ellipse-like suspen-dome and single-layer reticulated shell are all combinations of complex vibrations. Among them, the first and second vibration modes are mainly vertical vibrations with the participation of horizontal vibrations. The third and fourth modes are couplings of vertical vibrations and bending deformation.

Tab. 2 Frequencies and deflections of suspen-dome and single-layer reticulated shell

Modal	Frequency/Hz		Deflection
	Suspen-dome	Single-layer reticulated shell	
1	1.75	1.77	Anti-symmetric bending in lateral direction
2	2.05	2.08	Anti-symmetric bending in longitudinal direction
3	2.20	2.16	Anti-symmetric bending of inner and outer rings
4	2.30	2.25	High order anti-symmetric bending in lateral direction
5	2.32	2.35	Anti-symmetric bending in 45° direction
6	2.42	2.43	Anti-symmetric bending in lateral direction
7	2.46	2.47	Anti-symmetric bending in longitudinal direction
8	2.57	2.49	Anti-symmetric bending of inner and outer rings
9	2.77	2.64	Space symmetric bending
10	2.81	2.79	Salient in longitudinal direction
11	1.75	1.77	Space symmetric salient
12	2.05	2.08	Anti-symmetric salient in 45° direction

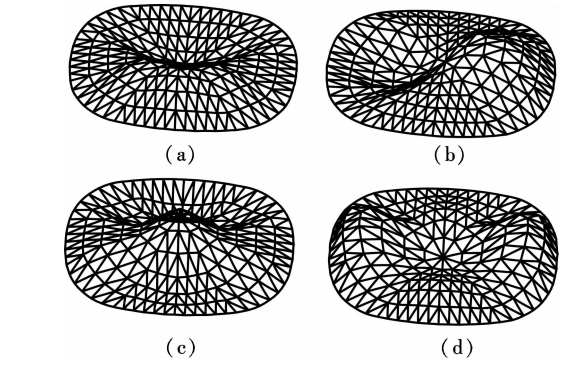

Fig. 4 Vibration modes of ellipse-like suspen-dome and single-layer reticulated shell. (a) First order; (b) Second order; (c) Third order; (d) Fourth order

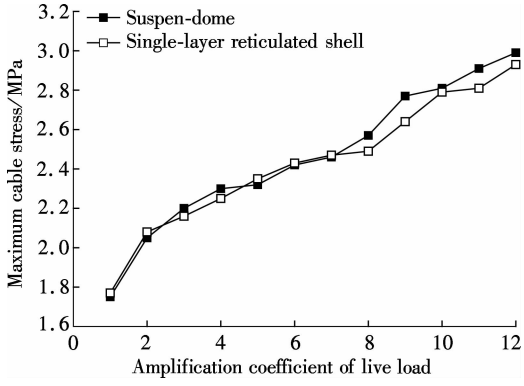

Fig. 5 Vibration mode-frequency curves of ellipse-like suspen-dome and single-layer reticulated shell

4 Overall Stability Analysis

4.1 Linear stability analysis

A linear ultimate live load coefficient is the product of designate load and buckling coefficient. By solving eigenvalue buckling modes, we find the linear buckling coefficient. To be specific, designated load includes dead load and live load. The dead load is applied at first, and then the live load. When the buckling coefficient is 1, the live load is ultimate linear load. By achieving the ultimate linear load, we find the ultimate live load coefficient of a certain live load arrangement, namely, the linear ultimate live load coefficient K_L.

Tab. 3, Fig. 6 and Fig. 7 show the linear ultimate live load coefficients and the ultimate first-order modal shapes of different live load arrangements. The results are listed as follows.

1) The arrangement of live load makes a great difference on linear buckling modes. Under different load arrangements, the reactions of K_L and buckling modes are different. The K_L of the lateral live load arrangement is relatively small, which means that it can easily cause overall buckling in the lateral direction.

2) The linear ultimate live loads of the ellipse-like suspen-dome and single-layer reticulated shell are uniform, and the bottom cable-strut system has little effect on the linear stability analysis.

3) The patterns of the first-order buckling modes of the

single-layer reticulated shell are similar to the arrangements of live load. However, the first-order buckling modes of all these three load arrangements of the suspen-dome are the rotation of the inner reticulated shell in the lateral direction, which means that the bottom cable-strut system greatly improves the in-plane stiffness of the inner region, and has great influence on the instability modes of the single-layer reticulated shell.

Tab. 3 Linear buckling live load coefficient K_L

Structure type	Full span	Longitudinal half-span	Lateral half-span
Suspen-dome	27.79	27.78	26.42
Single-layer reticulated shell	24.06	19.97	19.82

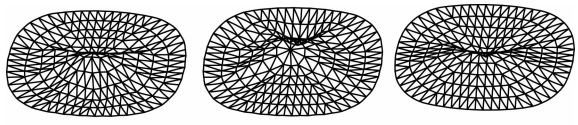

(a) (b) (c)

Fig. 6 First linear buckling modes of ellipse-like suspen-dome. (a) Full-span; (b) Longitudinal half-span; (c) Lateral half-span

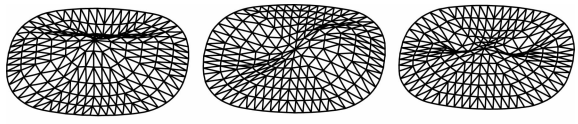

(a) (b) (c)

Fig. 7 First linear buckling modes of ellipse-like single-layer reticulated shell. (a) Full-span; (b) Longitudinal half-span; (c) Lateral half-span

4.2 Nonlinear stability analysis

Based on the consistent mode imperfection method[12], we conduct a nonlinear stability analysis under three different conditions: a) Geometric nonlinearity; b) Geometric nonlinearity with initial imperfection; c) Geometric nonlinearity, material nonlinearity with initial imperfection. Specifically, the nonlinear analysis principles are shown below.

1) When performing a geometric nonlinearity analysis, we consider the influences of large deformation and stress stiffening, and use the Newton-Raphson method to finish the iteration calculation.

2) When performing a material nonlinearity analysis, the yield strength and yield elastic modulus of oblique rods, cable hoops and other steel components are listed in Tab. 4.

3) The first-order vibration mode is taken as the distribution mode of initial imperfection, and the maximum value is l/300 length of the reticulated shell in the lateral direction (255 mm).

Tab. 4 Material parameters of components MPa

Component name	Elastic modulus	Yield strength	Yield elastic modulus	Ultimate strength
Oblique rods	2.06×10^5	650	1 333	850
Cable hoops	1.60×10^5	—	—	—
Others	2.06×10^5	345	6 180	490

Notes: "—" means not yielded.

Uniform live load and concentrated live load are multiplied to add on the roof of the suspen-dome or single-layer reticulated shell. When the overall structure is instable, the amplification coefficient of live load is the ultimate live load coefficient. Tab. 5 and Tab. 6 list the ultimate live load coefficients of the above three conditions, and Figs. 8 to 13 show the instability modes of different load arrangements, respectively. The curves of live load versus vertical deformation are shown in Fig. 14, and the curves of live load versus cable stress are shown in Fig. 15. The results are listed as follows.

1) The ultimate live loads and instability forms of the suspen-dome and single-layer reticulated shell are close when ignoring the effects of initial imperfection and material nonlinearity.

Tab. 5 Nonlinear ultimate live load coefficients of suspen-dome

Parameters	Geometric nonlinearity only			Geometric nonlinearity with initial imperfection			Geometric nonlinearity, material nonlinearity with initial imperfection		
	Full-span	Longitudinal half-span	Lateral half-span	Full-span	Longitudinal half-span	Lateral half-span	Full-span	Longitudinal half-span	Lateral half-span
Ultimate live load coefficient	18.8	19.2	17.8	15.5	14.4	12.9	10.2	9.9	9.2
Ultimate load coefficient	7.5	7.7	7.1	6.2	5.8	5.2	4.1	4.0	3.7
Maximum vertical displacement/mm	−424.5	−529.9	−864.3	−323.9	−675.3	−822.8	−205.4	−448.4	−402.6
Maximum equivalent stress/MPa	1 254.0	1 419.0	1 933.0	1 064.0	1 670.0	1 458.0	414.9	405.0	412.9
Maximum cable stress/MPa	545.4	527.6	573.0	505.7	492.0	489.1	451.7	450.6	455.2

Tab. 6 Nonlinear ultimate live load coefficients of single-layer reticulated shell

Parameters	Geometric nonlinearity only			Geometric nonlinearity with initial imperfection			Geometric nonlinearity, material nonlinearity with initial imperfection		
	Full-span	Longitudinal half-span	Lateral half-span	Full-span	Longitudinal half-span	Lateral half-span	Full-span	Longitudinal half-span	Lateral half-span
Ultimate live load coefficient	16.1	16.6	15.7	11.6	9.7	8.4	7.2	5.1	4.5
Ultimate load coefficient	6.4	6.6	6.3	4.6	3.9	3.4	2.9	2.0	1.8
Maximum vertical displacement/mm	−456.1	−529.3	−674.3	−488.2	−595.2	−701.9	−218.4	−309.1	−473.3
Maximum equivalent stress/MPa	1 252.0	1 314.0	1 325.0	1 197.0	1 509.0	1 194.0	402.8	478.6	406.5

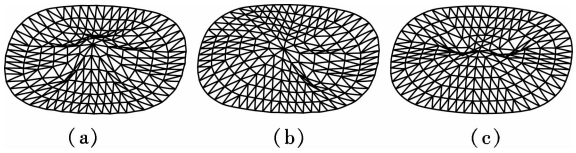

Fig. 8 Geometric nonlinear instability mode of suspen-dome without initial imperfection. (a) Full-span; (b) Longitudinal half-span; (c) Lateral half-span

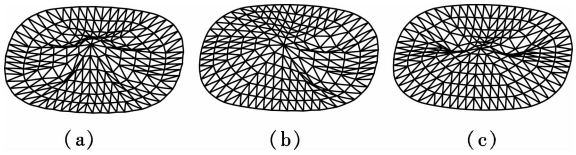

Fig. 9 Geometric nonlinear instability mode of single-layer reticulated shell without initial imperfection. (a) Full-span; (b) Longitudinal half-span; (c) Lateral half-span

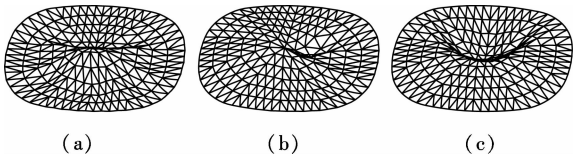

Fig. 10 Geometric nonlinear instability mode of suspen-dome with initial imperfection. (a) Full-span; (b) Longitudinal half-span; (c) Lateral half-span

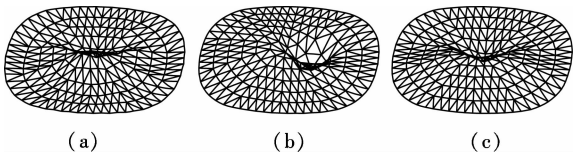

Fig. 11 Geometric nonlinear instability mode of single-layer reticulated shell with initial imperfection. (a) Full-span; (b) Longitudinal half-span; (c) Lateral half-span

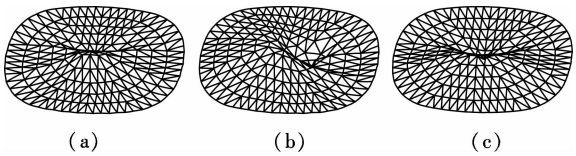

Fig. 12 Geometric-material nonlinear instability mode of suspen-dome with initial imperfection. (a) Full-span; (b) Longitudinal half-span; (c) Lateral half-span

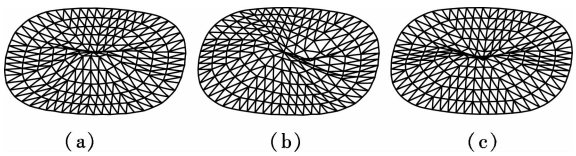

Fig. 13 Geometric-material nonlinear instability mode of single-layer reticulated shell with initial imperfection. (a) Full-span; (b) Longitudinal half-span; (c) Lateral half-span

2) The live load arrangement has great influence on structural stability. The ultimate live load coefficients of the lateral half-span live load arrangement are less than those of other situations for both the ellipse-like suspen-dome and single-layer reticulated shell. This suggests that the lateral half span live load arrangement is the most unfavorable situation.

3) Initial imperfection decreases the ultimate live load.

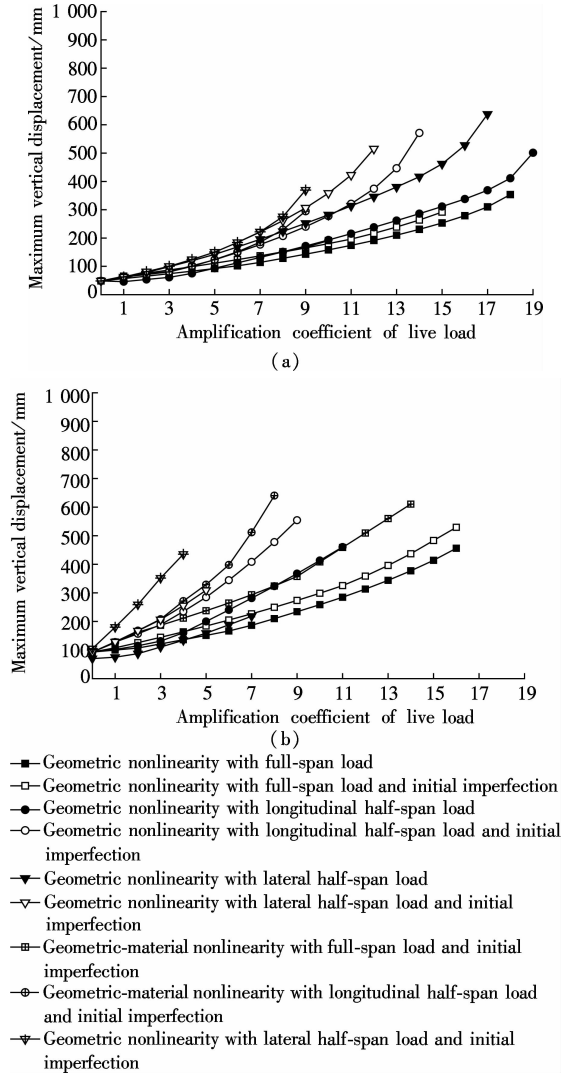

Fig. 14 Curves of live load vs. vertical deformation. (a) Suspen-dome; (b) Single-layer reticulated shell

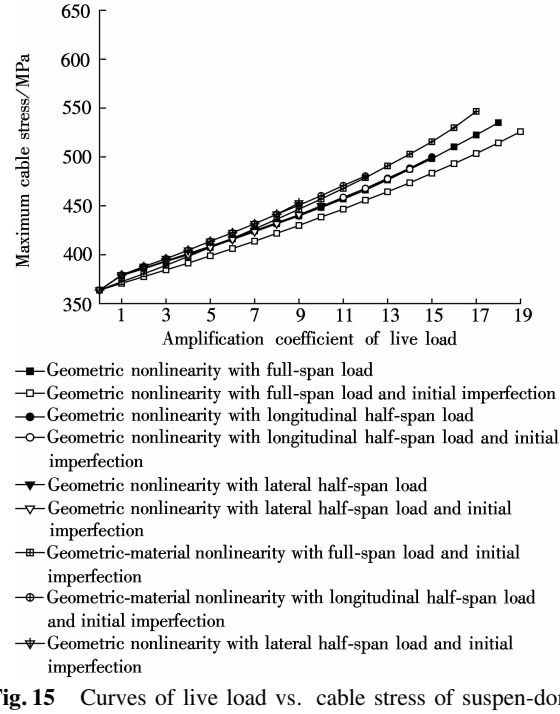

Fig. 15 Curves of live load vs. cable stress of suspen-dome

When the initial imperfection is added from 0 to 1/300, the ultimate live load coefficients of these three arrangements of the suspen-dome decrease from 18.8, 19.2 and 17.8 to 15.5, 14.4 and 12.9, respectively, which is a reduction of 17.6%, 25.0% and 27.5%. However, the ultimate live load coefficients of the single-layer reticulated shell decrease from 16.1, 16.6 and 15.7 to 11.6, 9.7 and 8.4, respectively, which is a reduction of 28.0%, 41.6% and 46.5%. It shows that a low rise-span ratio ellipse-like suspen-dome is sensitive to initial imperfection, and the bottom cable-strut system greatly improves the stability performance of the single-layer reticulated shell.

4) When considering material nonlinearity, the stability capacity experiences a significant reduction due to the parts of the components yielded. The ultimate live load coefficients of these three arrangements of the suspen-dome decrease from 15.5, 14.4 and 12.9 to 10.2, 9.9 and 9.2, respectively, when we consider both geometric nonlinearity and material nonlinearity, which is a reduction of 34.2%, 44.1% and 28.7%. The ultimate live load coefficients of the single-layer reticulated shell decrease from 11.6, 9.7 and 8.4 to 7.2, 5.1 and 4.5, respectively, which is a reduction of 37.9%, 47.4% and 46.4%. This indicates that material nonlinearity greatly reduces the ultimate bearing capacity of both the suspen-dome and single-layer reticulated shell. Therefore, it is necessary to take material nonlinearity into account when conducting a finite element analysis in order to ensure the structural safety.

5) Different from the regular circular or ellipse suspen-dome, the main instability modes of the ellipse-like suspen-dome and its single-layer reticulated shell behave deflection of bending at the loading area.

6) During a nonlinear instability analysis, some cables relax whereas some cables yield. However, the maximum cable force does not exceed its breaking force. Thus, the overall structure collapses before the single cable breaks.

7) In this project, the lowest nonlinear ultimate live load coefficients of the suspen-dome and single-layer reticulated shell are 9.2 and 4.5, respectively. The corresponding ratios between ultimate bearing capacity and designated vertical load ("ultimate load coefficient" in short) are 3.7 and 1.8, respectively. According to previous literature[13], this ratio K should be greater than 2.0. In this case, the suspen-dome is above the threshold value while the single-layer reticulated shell is instable when considering geometric nonlinearity, material nonlinearity and initial imperfection at the same time.

5 Conclusion

For low rise-span ratio suspen-domes, the bottom cable-strut system greatly increases the integrity of the whole structure and reduces the sensitivity of the single-layer reticulated shell to initial geometric imperfection, while it does not change much in integral rigidity, fundamental vibration frequencies, linear ultimate live loads, and geometric nonlinear ultimate live loads without initial imperfection. However, when considering material nonlinearity and initial imperfection, a great reduction occurs in the ultimate stability capacity. In this case, a lower rise-span ratio suspen-dome is sensitive to initial imperfection, and material nonlinearity should be taken into account to ensure the safety of the structure during stability analysis. For this project, stability is still one of the controlling factors in the designing process, and the overall structure will be unstable after removing the bottom cable-strut system. Moreover, the distribution patterns of the live load greatly influence the instability modes of the structure, and the uniform live load with full span is not always the most dangerous case.

References

[1] Kawaguchi M, Abe M, Hatato T, et al. On a structural system "suspen-dome" system [C]//*Proc of IASS Symposium*. Istanbul, Turkey, 1993: 523 − 530.

[2] Kawaguchi M, Abe M, Tatemichi I. Design, tests and realization of suspen-dome system [J]. *Journal of the International Association for Shell and Spatial Structures*, 1999, **40**(3): 179 − 192.

[3] Qu M H. Construction study and control techniques on long-span suspendome structures [D]. Nanjing: School of Civil Engineering, Southeast University, 2008. (in Chinese)

[4] Kawanuchi M. Structural tests of a full-size suspen dome system [C]//*Proceedings of IASS Symposium*. Atlanta, USA, 1994: 383 − 392.

[5] Li Z, Zhang Z, Dong S, et al. Construction sequence simulation of a practical suspen-dome in Jinan Olympic Center [J]. *Advanced Steel Construction*, 2012, **8**(1): 38 − 53.

[6] Liu H, Chen Z. Non-uniform thermal behaviour of suspen-dome with stacked arch structures [J]. *Advances in Structural Engineering*, 2013, **16**(6): 1001 − 1010.

[7] Guo Z X, Shi K R, Luo B, et al. Lifting installation and prestressed cable construction of cable-suspended reticulated shell of steel roof in Wuhan Gymnasium [J]. *Construction Technology*, 2006, **35**(12): 51 − 53, 58. (in Chinese)

[8] Cao Z G, Wu Y, Qian H L, et al. Design and analysis of giant grid suspen-dome of Dalian Centre Gymnasium [J]. *Steel Construction*, 2011, **26**(1): 37 − 42. DOI: 10.3969/j.issn.1007 − 9963.2011.01.008. (in Chinese)

[9] Kang W, Chen Z, Lam H F, et al. Analysis and design of the general and outmost-ring stiffened suspen-dome structures [J]. *Engineering Structures*, 2003, **25**(13): 1685 − 1695.

[10] Zhou Z, Wu J, Meng S. Influence of member geometric imperfection on geometrically nonlinear buckling and seismic performance of suspen-dome structures [J]. *International Journal of Structural Stability and Dynamics*, 2014, **14**(3): 193 − 224. DOI: 10.1142/S0219455413500703.

[11] Liu H J, Yang L F, Luo Y F. Dynamic stability of large-

span suspen-domes subjected to seismic excitations [J]. *Advanced Materials Research*, 2012, **378－379**: 209－212.

[12] Fan F, Yan J C, Cao Z G. Stability of single-layer reticulated domes with initial imperfection to members [J]. *Journal of Southeast University* (*Natural Science Edition*), 2009, **39**(S2): 158－164. (in Chinese)

[13] China Academy of Building Research. JGJ7—2010 Technical specification for space frame structures [S]. Beijing: China Architecture & Building Press, 2010. (in Chinese)

低矢跨比类椭圆形弦支穹顶结构稳定性能分析

丁明珉　罗　斌　陈项南　郭正兴　管东芝

(东南大学混凝土及预应力混凝土教育部重点实验室, 南京 210096)
(东南大学国家预应力工程技术研究中心, 南京 210096)

摘要: 为了研究初始几何缺陷和材料非线性对弦支穹顶稳定性分析的影响,以江苏文化城体育馆类椭圆形弦支穹顶为算例,进行了模态分析. 然后,对弦支穹顶与单层网壳进行了稳定性能对比研究,包括线性屈曲、几何非线性屈曲、考虑初始几何缺陷的几何非线性屈曲以及同时考虑几何-材料非线性的双非线性屈曲. 结果表明,索杆系增加了弦支穹顶的整体性,降低了单层网壳对初始几何缺陷的敏感性,但对结构刚度、自振频率、线性屈曲荷载、无初始缺陷的非线性屈曲荷载等影响不大. 当考虑初始几何缺陷和材料非线性时,2 种结构的极限稳定承载能力均大幅下降,表明低矢跨比弦支穹顶对初始几何缺陷和材料非线性较为敏感. 此外,活载分布模式对结构失稳模态影响较大,满跨活载并不一定是最不利的活载分布模式.

关键词: 弦支穹顶;单层网壳;类椭圆形;稳定性分析;初始几何缺陷;几何非线性;材料非线性

中图分类号: TU393. 3